The Universe Viewed in Gamma-Rays

Sept. 25-28, 2002

ICRR, Univ. Tokyo

why high energy γ-rays ?

* origin of cosmic rays
* characteristics of cosmic ray sources
* physics of particle acceleration
* something new

the number of confirmed sources

— only handful sources observed

* PWN Crab, PSR1706, Vela
* SNR SN1006, RX J1713.7, Cas A
* Blazars Mkn421, Mkn501, PKS2155, 1ES1426, 1ES1959, 1ES2344

No positive identifications with

Pulsars, X-ray stars, GRBs, ----

◎ PWN

Slane, de Jager, Shibata

HST & Chandra Monitoring of the Crab Nebula

{ Time dependent structure changes
{ Spatially resolved structure

wisp movement with ~0.5c

polar jet, knots, ----

Is the standard model (Kennel & Coroniti (1984)) still viable or does it need substantial modification?

$\sigma \sim 10^{-3}$, $\Gamma \sim 10^{7}$ $e^{\pm}$ wind

relativistic MHD shock at ~0.2pc

3-D structure (Shibata)

(larger σ
(smaller Γ
(post-shock bulk acceleration ?

◎ SNR   Tanimori, Berezhko, Bamba

RX J1713.7−3946

Evidence for proton acceleration ?

* steep sub-TeV spectrum suggests
  π^0-decay γ-rays rather than IC. (Tanimori)
* TeV spectral shape does not show
  good match with that of GCR
  low Emax, high Emin
  or steeper spectrum than GCR
* Inhomogeneous B is a possible solution
  with IC model (Slane).

SN1006

e^- IC interpretation

Chandra spatial structure
thin filaments ⇒ small X implies "Perpendicular Shock"

Effects of inhomogeneities in
e^- acceleration. B-field and others

Hadronic (Berezhko) vs Leptonic remains
to be settled.

Implications for particle acceleration processes

Hoshino, Schlickeiser

beyond the standard Fermi shock acceleration

- Too low Emax To explain the knee
* non-linear effects predict deviation
  from a power law spectrum
* acceleration efficiency of protons
  may be low from observed upper
  limits of TeV photons

----

internal E-field structure of high
Mach number perpendicular shocks

efficient electron acceleration
by surfing mechanism

{ spectral shape ?
{ anisotropy strong ?

5

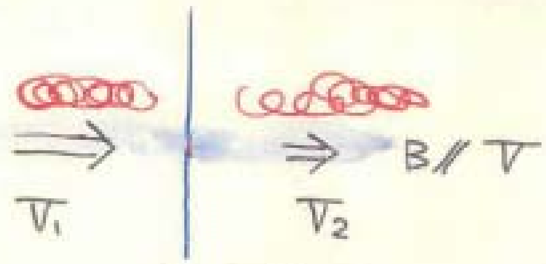

shock front

shock acceleration by parallel shock

acceleration by E-field of scattering MHD waves

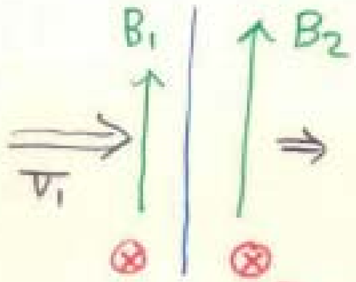

$$E = \frac{VB}{c}$$

motional E-field

e^- trapping at the soliton

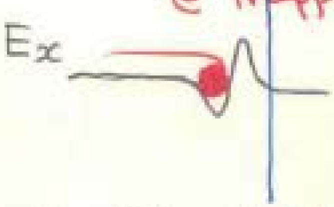

acceleration by motional E-field

soliton like structure

6

- Blazars   Coppi, Mukherjee

internal shock model in relativistic jets

energetics, acceleration of electrons

jet formation mechanism ----

observational confrontation

multi-TeV γ-rays from Mkn421/501

and intergalactic absorption

Dwek

m.f.p.

$$\sim 40\ \mathrm{Mpc}\left(\frac{10\,\mathrm{TeV}}{E}\right)\cdot\left(\frac{10\ \mathrm{nW\,m^{-2}\,sr^{-1}}}{I}\right)$$

details depend on the spectral shape

observations of diffuse IR background

K-band 20 ± 6 nW m^{-2} sr^{-1}

vs

direct count of faint galaxies at Subaru deep field

K-band $7.8 \sim 10.2$ nW m^{-2} sr^{-1}

(Totani et al. 2001)

Dwek; convergence to relatively low

$\nu I_\nu \sim 5\text{–}10$ nW $m^{-2} sr^{-1}$

cutoff energy of Mkn 421/501

~ 3–6 TeV

common or different for the two sources?

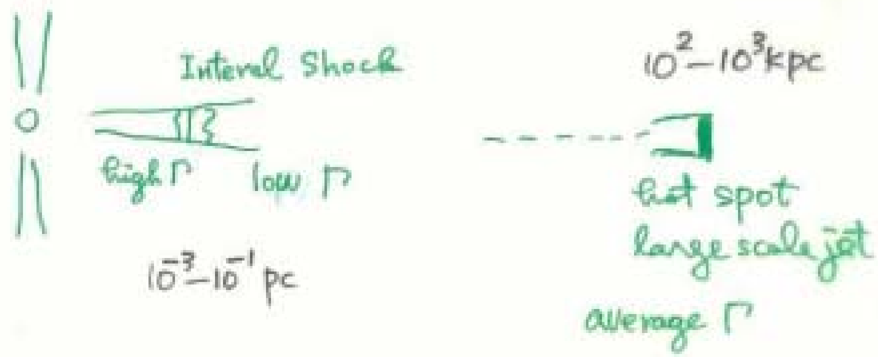

* basic model is correct

* details unknown

simple one-zone SSC model

successes & inadequencies

{ inhomogeneities
time dependence
environment (Ext. soft photons
deceleration mechanisms
---)

◎ other categories

galactic disk — Pohl

clusters of galaxies — Völk, Miniati

star burst galaxies — NGC253 (Cangaroo II)

extragalactic background — Pavlidou

GRB — SSP (Bergström)

X-ray binaries

Pulsars

New Large Facilities of TeV observation
(Veritas Hess Magic Cangaroo III)

GLAST

X-ray, radio, optical/multi-wavelength

expect more surprises as well as increasing number of TeV sources in the coming years

nature letters to nature

Close this window to return to the previous window

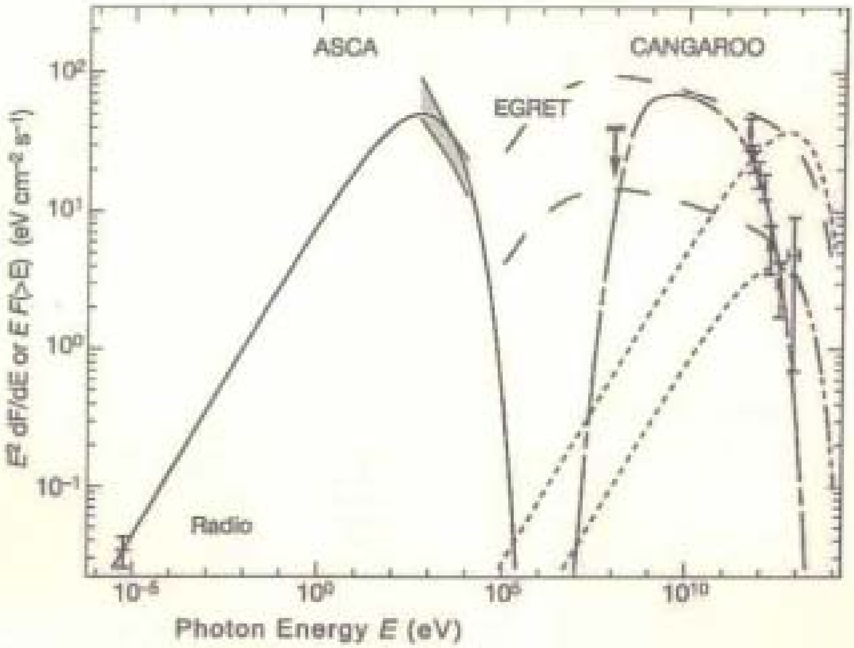

Figure 2 Multi-band emission from RX J1713.7−3946, and emission models. The radio observation was made with ATCA[19]. The ATCA flux at 1.36 GHz is estimated from two bright filaments lying in the northwest rim of RX J1713.7−3946 to be $S = 4 \pm 1$ Jy (ref. 19). The shaded area between the thick lines indicates the X-ray emission measured by the GIS detector on the ASCA satellite[17]. The integral flux between 0.5 and 10.0 keV was obtained from Table 4.5 in ref. 17 and the spectral index in Table 4.4. The differential flux was calculated from these two values at 3 keV, the mean GIS sensitivity. The flux uncertainty due to the extended structure of the source was considered to be within +10%/−30%, which was calculated following the procedure described in ref. 29. The EGRET upper limit corresponds to the flux of 3EG J1714−3857[20]. The TeV γ-ray points are from this work (CANGAROO). Lines show model calculations: synchrotron emission (solid line), inverse Compton emission (dotted lines), bremsstrahlung (dashed lines) and emission from π^0 decay (short-long dashed line). Inverse Compton emission and bremsstrahlung are plotted for two cases: 3 μG (upper curves) and 10 μG (lower curves). The distance to this SNR has ambiguity as follows: the rotation velocity of the associated molecular cloud from this observation yielded a distance to the SNR of 6 ± 1 kpc, in contrast to the distance of 1 kpc estimated from soft-X-ray absorption[2]. The age for the SNR is estimated to be more than 10,000 yr (for a distance of 6 kpc) or ~2,000 yr (for 1 kpc). Details of these models are given in the text.

⟵ Item ⟶

Note: Figures may be difficult to render in a web browser. In such cases, we recommend downloading the PDF version of this document.

Hester et al. (2002)

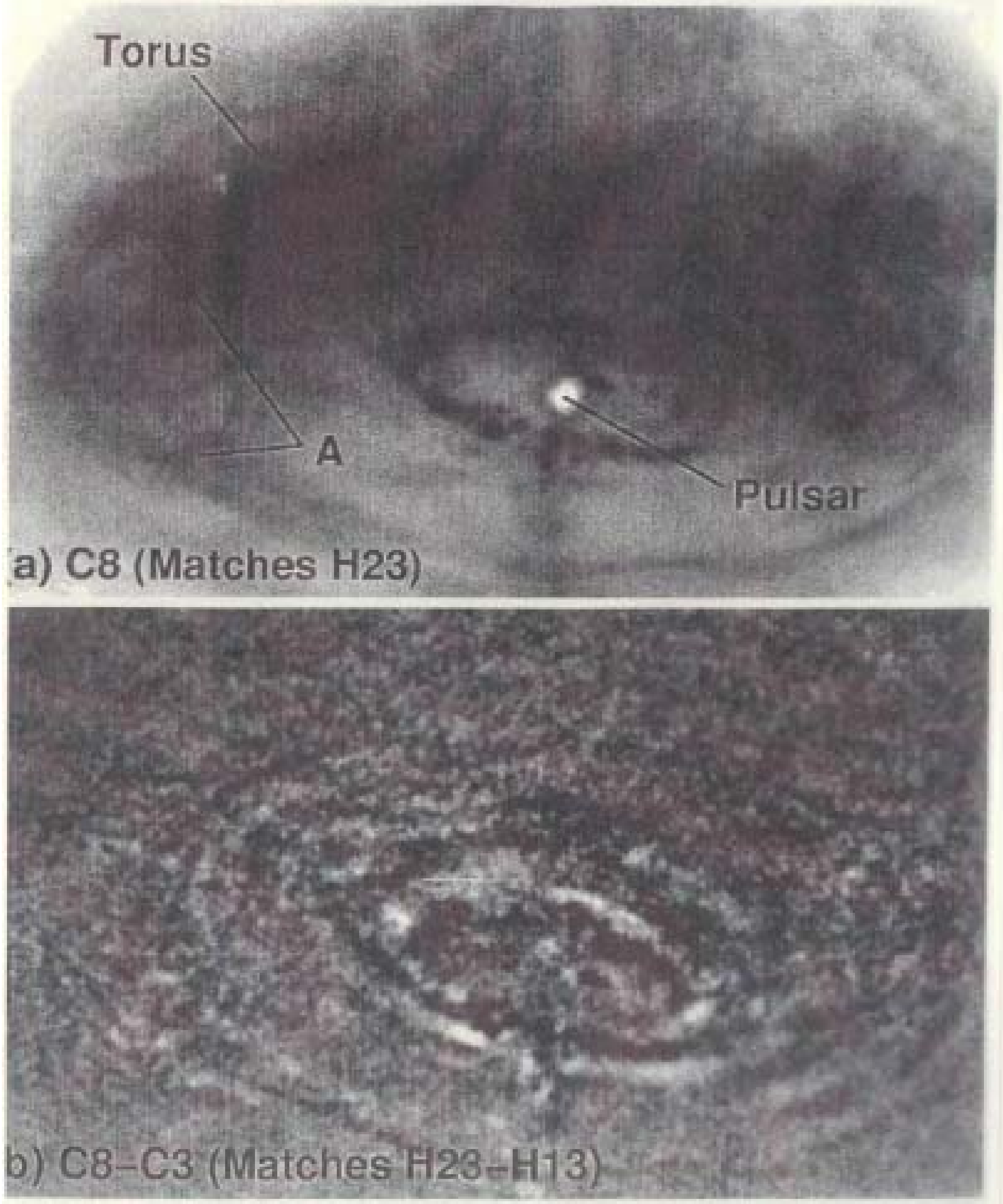

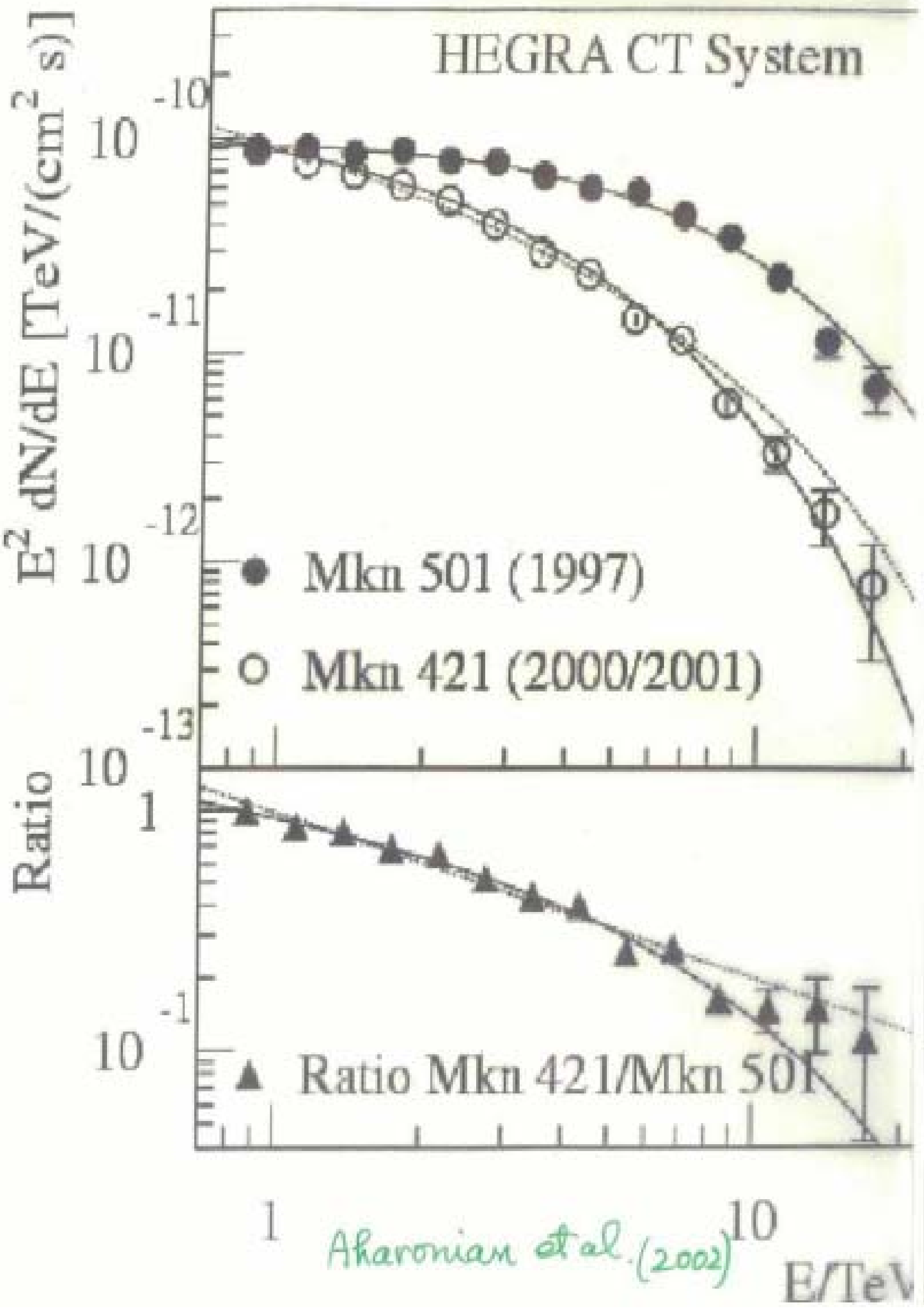
HEGRA CT System
E^2 dN/dE [TeV/(cm^2 s)]
Mkn 501 (1997)
Mkn 421 (2000/2001)
Ratio
Ratio Mkn 421/Mkn 501
E/TeV
Aharonian et al. (2002)

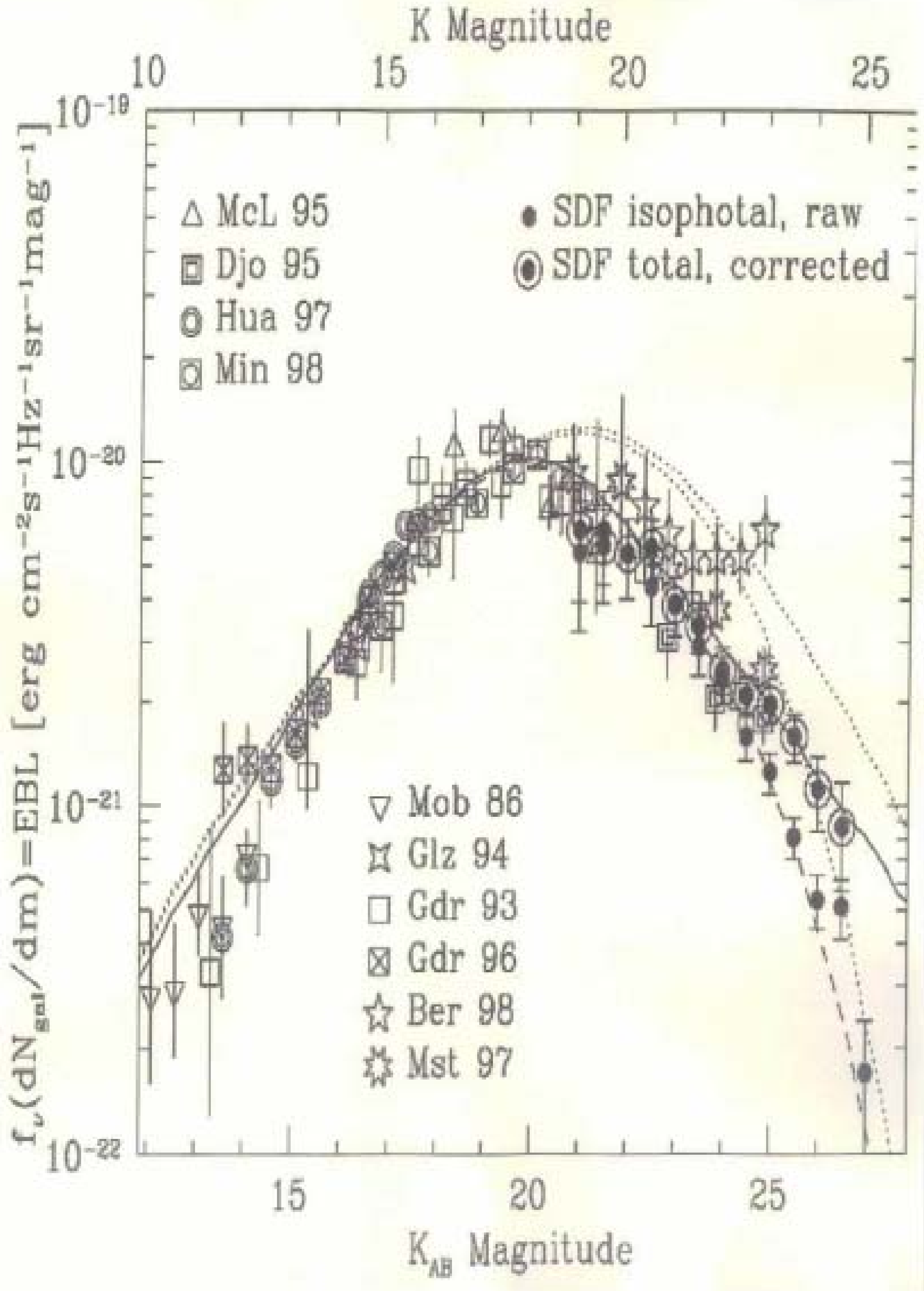
K Magnitude
f_ν(dN_gal/dm)=EBL [erg cm^-2s^-1Hz^-1sr^-1mag^-1]
McL 95
Djo 95
Hua 97
Min 98
SDF isophotal, raw
SDF total, corrected
Mob 86
Glz 94
Gdr 93
Gdr 96
Ber 98
Mst 97
K_AB Magnitude

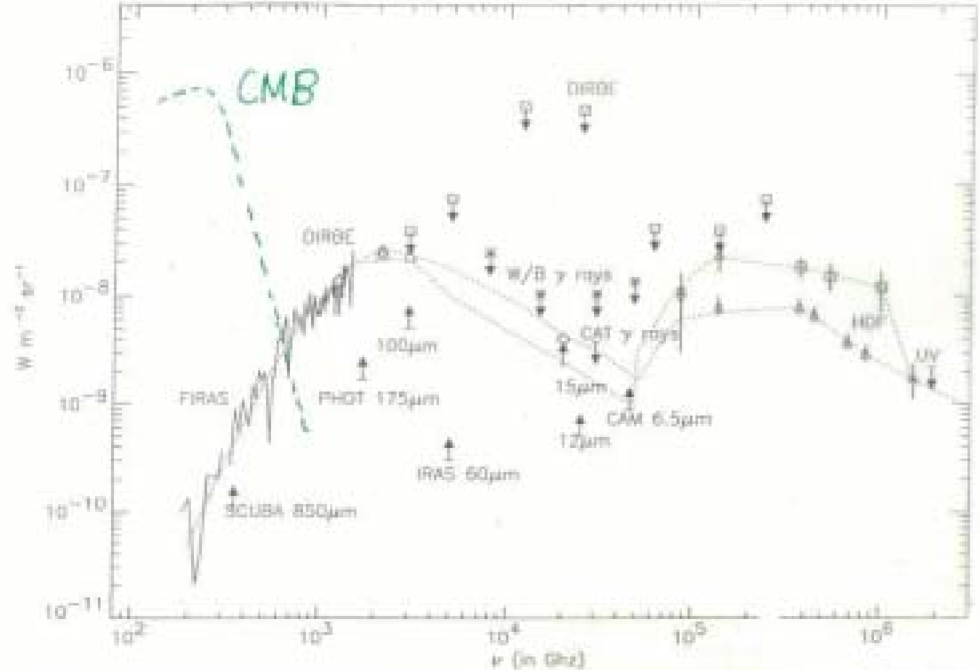

Fig. 1. Cosmic Background from the UV to the millimeter wavelength. In the UV domain, the upper limit is from Martin et al. (1991) and the value from Armand et al. (1994); the optical and near-IR points are from Pozzetti et al. (1998) (triangles) and Bernstein et al., in preparation (squares). The 3.5 and 2.2 μm points are from Dwek & Arendt (1998) and Gorjian et al. (2000); Squared upper limits are from Hauser et al. (1998) and crossed upper limits from Biller et al. (1998); the upper limit "CAT" is from Barrau (1998) and Barrau et al., in preparation. The 6.5 (Désert, private communication), 12 (Clements et al. 1999) and 15 μm (Elbaz et al. 1999) lower limits come from ISOCAM number counts; the value at 15 μm (c) is an extrapolation of the counts using the Guiderdoni et al. (1998) model. At longer wavelength, we have the 100, 140 and 240 μm Lagache et al. (2000) (△) and Hauser et al. (1998) (o) DIRBE values, lower limit from Dwek et al. (1998), upper limits from number counts at 60 (Lonsdale et al. 1990), 175 (Puget et al. 1999) and 850 μm (Barger et al. 1999). Dotted lines are an attempt to draw continuous lines compatible with all available data which then can be used for estimating the energy contribution of a given wavelength range.

CIB

Totani et al. (2001)

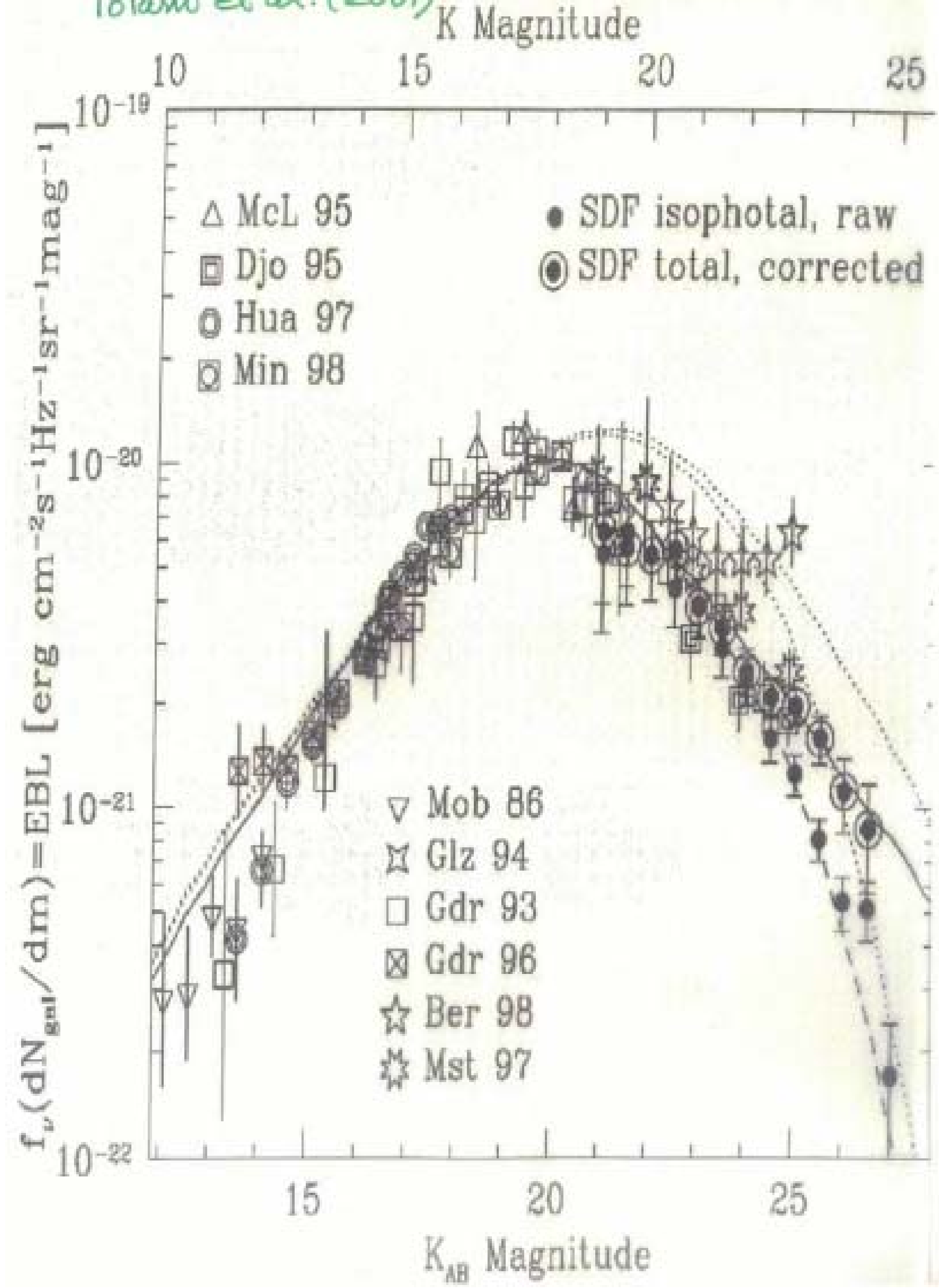

Enomoto et al (2002)

nature letters to nature

Close this window to return to the previous window

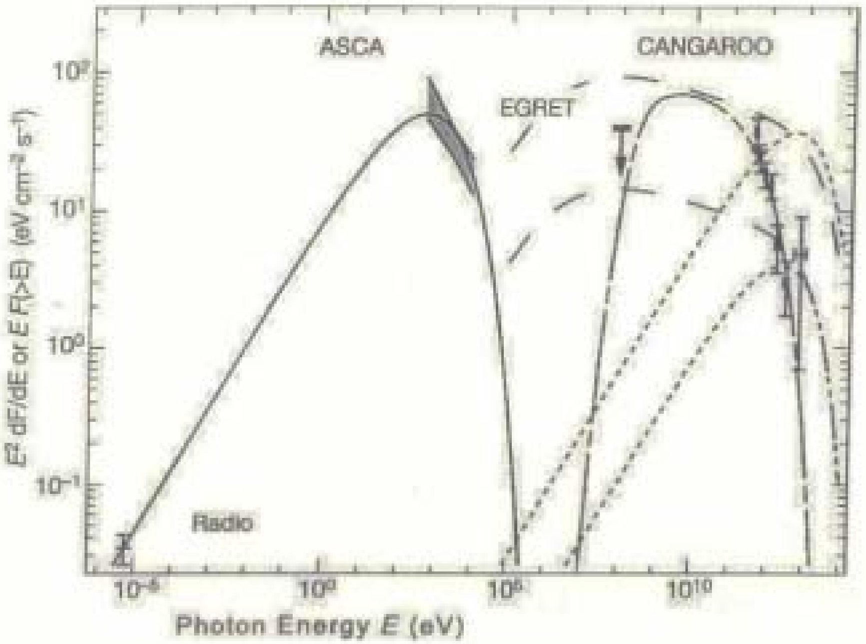

Figure 2 Multi-band emission from RX J1713.7−3946, and emission models. The radio observation was made with ATCA[19]. The ATCA flux at 1.36 GHz is estimated from two bright filaments lying in the northwest rim of RX J1713.7−3946 to be $S = 4 \pm 1$ Jy (ref. 19). The shaded area between the thick lines indicates the X-ray emission measured by the GIS detector on the ASCA satellite[17]. The integral flux between 0.5 and 10.0 keV was obtained from Table 4.5 in ref. 17 and the spectral index in Table 4.4. The differential flux was calculated from these two values at 3 keV, the mean GIS sensitivity. The flux uncertainty due to the extended structure of the source was considered to be within +10%/−30%, which was calculated following the procedure described in ref. 29. The EGRET upper limit corresponds to the flux of 3EG J1714−3857[30]. The TeV γ-ray points are from this work (CANGAROO). Lines show model calculations: synchrotron emission (solid line), inverse Compton emission (dotted lines), bremsstrahlung (dashed lines) and emission from π^0 decay (short–long dashed line). Inverse Compton emission and bremsstrahlung are plotted for two cases: 3 μG (upper curves) and 10 μG (lower curves). The distance to this SNR has ambiguity as follows: the rotation velocity of the associated molecular cloud from this observation yielded a distance to the SNR of 6 ± 1 kpc, in contrast to the distance of 1 kpc estimated from soft-X-ray absorption[8]. The age for the SNR is estimated to be more than 10,000 yr (for a distance of 6 kpc) or ~2,000 yr (for 1 kpc). Details of these models are given in the text.

⟵ Item ⟶

Note: Figures may be difficult to render in a web browser. In such cases, we recommend downloading the PDF version of this document.